Supplementary material for the manuscript:

A platform for constructing, evaluating, and screening bioconjugates on the yeast surface

James A. Van Deventer[1,2,3,*], Doris N. Le[2,3], Jessie Zhao[2,3], Haixing P. Kehoe[1], and Ryan L. Kelly[2,4]

[1]Chemical and Biological Engineering Department, Tufts University, 4 Colby Street Room 148, Medford, MA 02155, United States of America, [2]Koch Institute for Integrative Cancer Research, [3]Department of Chemical Engineering, and [4]Department of Biological Engineering, Massachusetts Institute of Technology, 500 Main Street, Building 76 Room 289, Cambridge, MA 02139, United States of America

*To whom correspondence should be addressed. Email: James.Van_Deventer@tufts.edu

Table SI. Median fluorescence values of reporter and control scFv-Fc constructs induced in cells expressing aminoacyl-tRNA synthetase (aaRS) variants in culture media supplemented with indicated ncAAs.

Reporter Construct	aaRS	ncAA	Cells Displaying Construct (Q2)		Nondisplaying Cells (Q4)		Total Population (All Quadrants)		Percent Displaying Cells (Q2)	Ratio of percent displaying cells –ncAA/ncAA[a]
			MFI Cmyc	MFI HA	MFI Cmyc	MFI HA	MFI Cmyc	MFI HA		
scFv-Fc-TAG-Aga2p	AzFRS	AzF	8.93E+03	2.28E+04	2.33E+02	1.70E+03	8.44E+02	5.42E+03	46.0	0.235
scFv-Fc-TAG-Aga2p	AzFRS	AcF	6.00E+03	1.55E+04	2.30E+02	1.55E+03	4.41E+02	2.72E+03	28.1	0.384
scFv-Fc-TAG-Aga2p	AzFRS	OmeY	3.98E+03	1.75E+04	2.49E+02	1.71E+03	4.96E+02	3.45E+03	32.9	0.328
scFv-Fc-TAG-Aga2p	AzFRS	None	1.96E+03	9.85E+03	2.39E+02	1.56E+03	3.13E+02	1.94E+03	10.8	NA
scFv-Fc-TAG-Aga2p	AcFRS	AzF	9.65E+03	2.84E+04	2.29E+02	1.36E+03	1.30E+03	8.79E+03	53.0	0.0602
scFv-Fc-TAG-Aga2p	AcFRS	AcF	1.20E+04	3.11E+04	2.45E+02	1.39E+03	1.73E+03	1.01E+04	55.6	0.0574
scFv-Fc-TAG-Aga2p	AcFRS	OmeY	8.04E+03	2.72E+04	2.48E+02	1.44E+03	1.02E+03	7.75E+03	50.8	0.0628
scFv-Fc-TAG-Aga2p	AcFRS	None	1.10E+03	8.58E+03	2.26E+02	1.32E+03	2.51E+02	1.47E+03	3.19	NA
scFv-Fc-TAG-Aga2p	OmeRS	AzF	6.67E+03	1.87E+04	2.49E+02	1.48E+03	7.69E+02	4.48E+03	44.4	0.234
scFv-Fc-TAG-Aga2p	OmeRS	AcF	2.58E+03	1.32E+04	2.42E+02	1.47E+03	3.16E+02	1.86E+03	13.2	0.788
scFv-Fc-TAG-Aga2p	OmeRS	OmeY	6.70E+03	2.05E+04	2.52E+02	1.54E+03	7.78E+02	4.88E+03	45.3	0.230
scFv-Fc-TAG-Aga2p	OmeRS	None	2.03E+03	1.24E+04	2.30E+02	1.44E+03	2.77E+02	1.74E+03	10.4	NA
scFv-Fc-Aga2p	None	None	5.51E+04	7.00E+04	1.75E+02	9.61E+02	3.30E+04	4.86E+04	79.0	NA

[a]The "Ratio of percent displaying cells –ncAA/ncAA" is calculated for a given aaRS and ncAA by dividing the percent of displaying cells observed after induction in the absence of ncAA by the percent of displaying cells observed after induction in the presence of ncAA. This ratio should be considered an estimate of the "worst-case" percentage of constructs displaying proteins containing canonical amino acids after induction in media containing ncAA. In reality, the high concentration of ncAA in the induction media is likely to reduce competition from canonical amino acids for activation by the "orthogonal" aaRS expressed in cells.

Table SII. Median fluorescence values of samples subjected to CuAAC evaluated before and after DTT treatment.

	Median Fluorescence Intensity (AU)[a]		
Sample	**Displaying cells (pre-DTT)**	**Nondisplaying cells (pre-DTT)**	**DTT-treated cells**
Fc no chemistry	267.7 ± 2.9	159.7 ± 5.3	180.3 ± 2.1
Fc CuAAC 20 μM **3**	274.7 ± 3.7	164.3 ± 5.2	205.0 ± 5.1
Fc SPAAC 10 μM **6**	306.7 ± 6.2	173.3 ± 5.2	248.7 ± 5.9
Fc 400 AzF no chemistry	361.7 ± 4.5	209.0 ± 2.2	227.7 ± 4.9
Fc 400 AzF CuAAC 20 μM **3**	628.3 ± 16.0	236.7 ± 1.2	335.7 ± 6.1
Fc 400 AzF SPAAC 10 μM **6**	492.3 ± 3.3	229.3 ± 0.5	326.7 ± 6.9

[a]Fluorescence values are reported as the average plus or minus the standard deviation of biotin fluorescence detected in triplicate experiments.

Table SIII. Midpoints of thermal denaturation of samples subjected to CuAAC.

Sample	$T_{1/2}$[a]
Fc no chemistry	65.65 ± 0.38[b]
Fc CuAAC no alkyne	68.11 ± 0.38
Fc CuAAC 20 μM **3**	66.74 ± 0.31
Fc 400 AzF no chemistry	63.85 ± 0.63
Fc 400 AzF CuAAC no alkyne	64.02 ± 1.12
Fc 400 AzF CuAAC 20 μM **3**	64.55 ± 0.75

[a]Midpoint of thermal denaturation.
[b]All reported errors are 95% confidence intervals of triplicate measurements of thermal denaturations.

Table SIV. Midpoints of thermal denaturation of samples subjected to SPAAC.

Sample	$T_{1/2}$[a]
Fc no chemistry	68.04 ± 0.16[b]
Fc SPAAC 10 μM **6**	68.60 ± 0.83
Fc 282 AzF no chemistry	66.37 ± 0.56
Fc 282 AzF SPAAC 10 μM **6**	65.59 ± 0.71
Fc 375 AzF no chemistry	67.71 ± 0.35
Fc 375 AzF SPAAC 10 μM **6**	67.64 ± 0.48
Fc 400 AzF no chemistry	66.54 ± 0.22
Fc 400 AzF SPAAC 10 mM **6**	66.08 ± 0.79

[a]Midpoint of thermal denaturation.
[b]All reported errors are 95% confidence intervals of triplicate measurements of thermal denaturations.

Table SV. Median fluorescence values of samples evaluated in two-step CuAAC detection reactions.

Sample	Median Fluorescence Intensity (AU)
Fc: 1) 20 μM **3**	200.3 ± 30.1
Fc 400 AzF: 1) 20 μM **3**	442.0 ± 81.6
Fc: 1) 0 μM **4**; 2) 20 μM **3**	213.3 ± 36.5
Fc 400 AzF: 1) 400 μM **4**; 2) 20 μM **3**	254.3 ± 19.7
Fc 400 AzF: 1) 100 μM **4**; 2) 20 μM **3**	315.3 ± 26.4
Fc 400 AzF: 1) 20 μM **4**; 2) 20 μM **3**	403.0 ± 31.2
Fc 400 AzF: 1) 0 μM **4**; 2) 20 μM **3**	459.3 ± 27.5

Table SVI. Median fluorescence values of samples evaluated in two-step SPAAC detection reactions.

Sample	Median Fluorescence Intensity (AU)
Fc: 1) 10 μM **6**	247
Fc 400 AzF: 1) 10 μM **6**	437
Fc: 1) 800 μM **7**; 2) 10 μM **6**	198
Fc: 1) 200 μM **7**; 2) 10 μM **6**	225
Fc 400 AzF: 1) 800 μM **7**; 2) 10 μM **6**	290
Fc 400 AzF: 1) 200 μM **7**; 2) 10 μM **6**	338

Table SVII. Observed fractions of Fc 400 TAG cells and corresponding calculated enrichment ratios in model sorting experiments.

Initial sample ratios	Fraction Fc 400 TAG in enriched outputs	Fold enrichment
100 Fc : 1 Fc 400 AzF	0.917 ± 0.018	91.7 ± 1.8
1,000 Fc : 1 Fc 400 AzF	0.134 ± 0.013	134 ± 13
10,000 Fc : 1 Fc 400 AzF	0.0102 ± 0.0098	102 ± 10

Table SVIII. Flow cytometry labeling conditions.

Detection	Primary label (dilution/concentration)	Secondary label (dilution)
Folded Fc	FcγRI (≥10.3 nM)	Rabbit anti-His FITC (1:200)
Biotin	None	Streptavidin Alexa Fluor 488 (1:200 (analysis) or 1:100 (sorting))
Fc display	Mouse anti-Xpress (1:1000−1:200 (analysis) or 1:400 (sorting))	Goat anti-mouse 647 (1:500) or goat anti-mouse 405 (1:200)
Cmyc tag	Chicken anti-Cmyc (1:250)	Goat anti-chicken 647 (1:100)
HA tag	Mouse anti-HA (1:200)	Goat anti-mouse 488 (1:100)

Supplementary Figures.

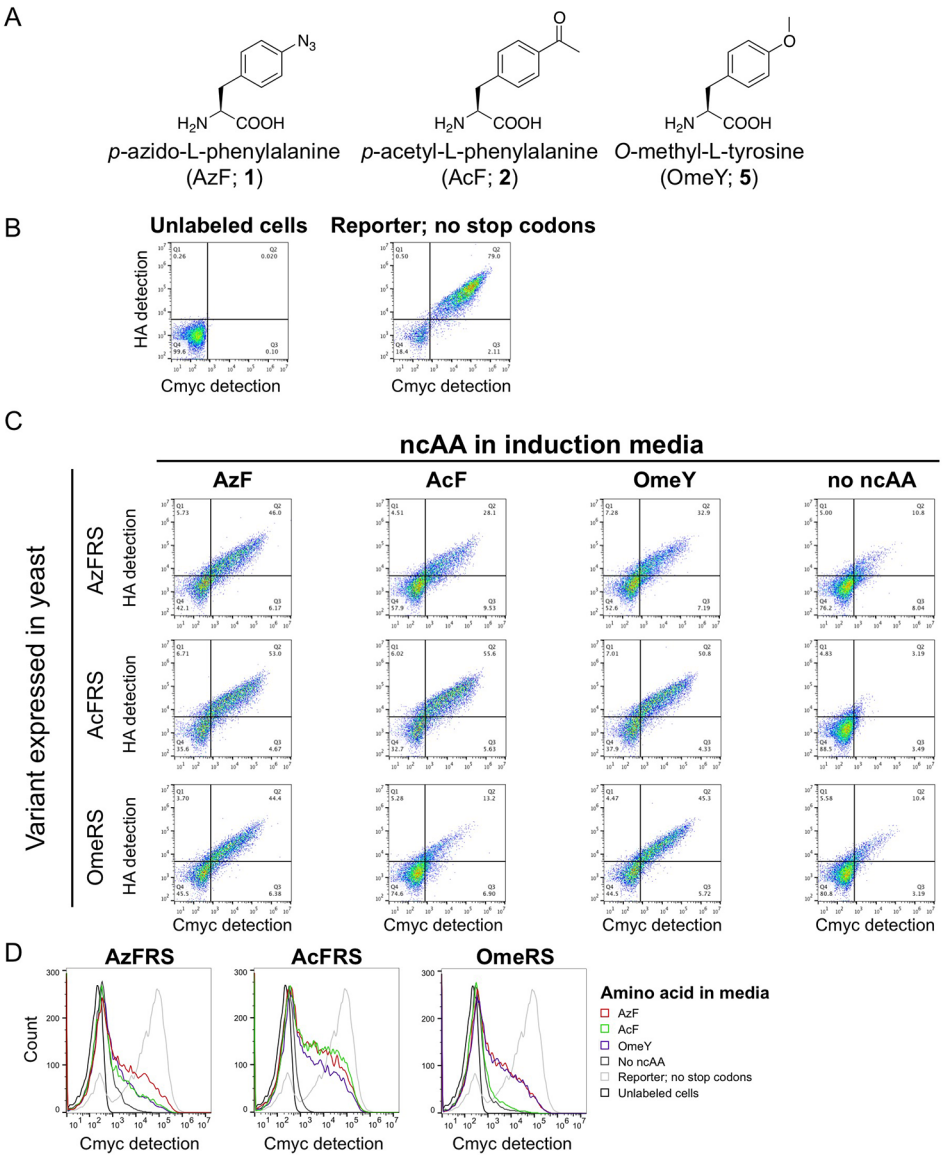

Fig. S1. Reporter system with expanded ncAA and aaRS variant data. (**A**) ncAAs used in study. (**B**) Control reporter construct experiments. Protein display levels with a plasmid encoding a reporter construct without an amber codon are higher than those observed when amber suppression is required for full-length protein display. (**C**) Flow cytometry analysis of reporter protein display levels detected via labeling of the Cmyc and HA epitope tags. Prior to detection, cultures were induced in media supplemented with 1 mM of the “L” form of a ncAA or no ncAA.

(**D**) Overlays of histograms comparing Cmyc detection levels from the data depicted in (**B**) and (**C**) grouped by aaRS.

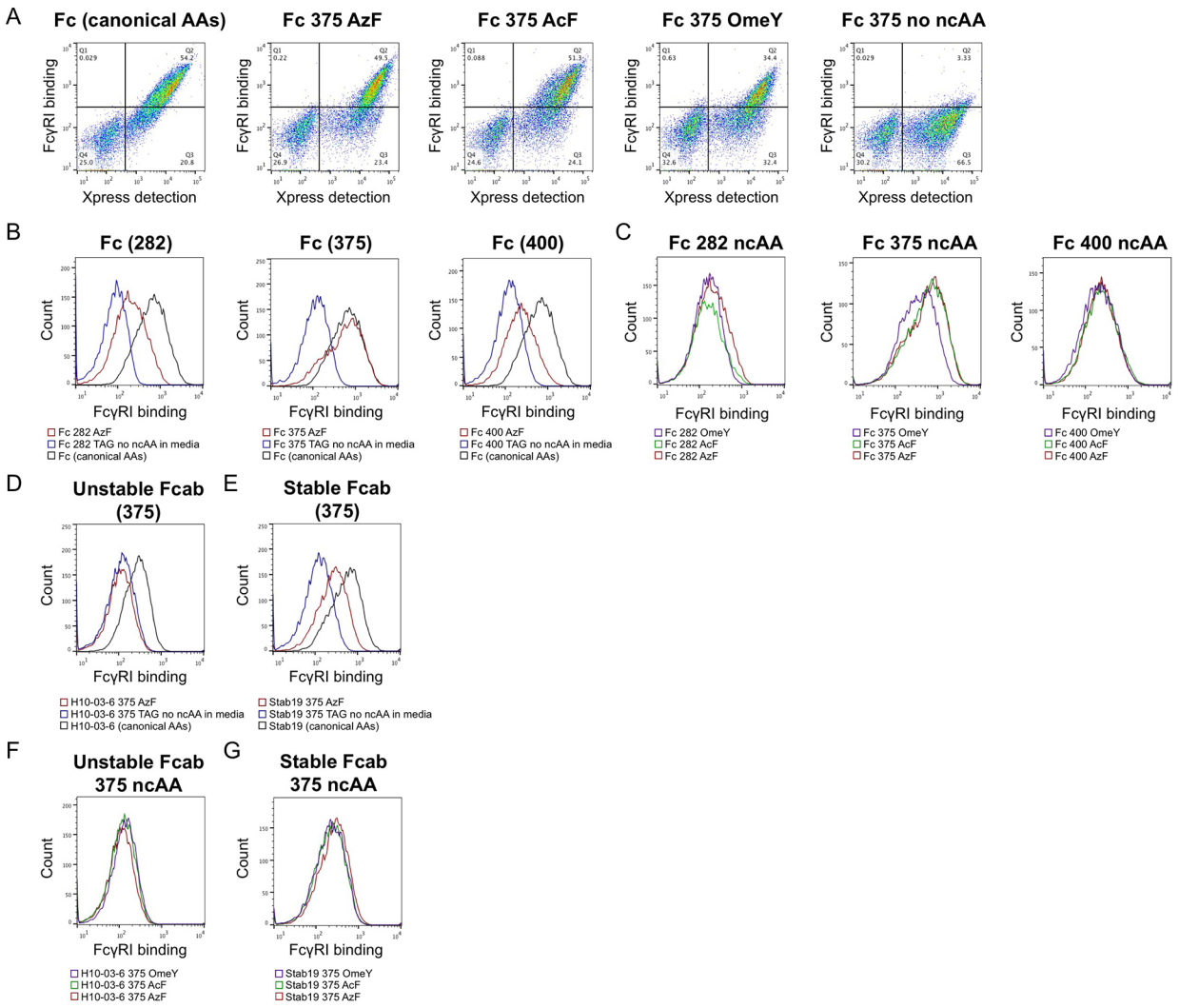

Fig. S2. Expanded studies of the properties of Fcs and Fcabs after ncAA substitution. (**A**) Representative dot plots from the detection of folded Fcs on the yeast surface for samples encoding an amber codon at position 375 and induced in media containing 1 mM final concentration of the indicated ncAA or no ncAA. (**B**) Detection of folded Fcs on the yeast surface after substitution with ncAAs at several substitution locations using the conformation-specific ligand FcγRI. Incorporating ncAAs at positions 282 and 400 results in a reduction of the amount of folded Fc detected on the yeast surface. (**C**) Effect of the incorporation of different ncAAs on FcγRI binding levels at several substitution positions. In general, different ncAA substitutions at the same position result in similar levels of FcγRI binding. (**D**)–(**G**) Studying

FcγRI binding of ncAA-substituted Fcabs. The incorporation of ncAAs causes loss of FcγRI binding in the unstable Fcab H10-03-6, but not the stable Fcab Stab19. Panels (**D**) and (**E**) are taken from Figure 2C and D, respectively, and are shown here for reference. (**F**), (**G**) Effects of the incorporation of different ncAAs at position 375 on FcγRI binding levels.

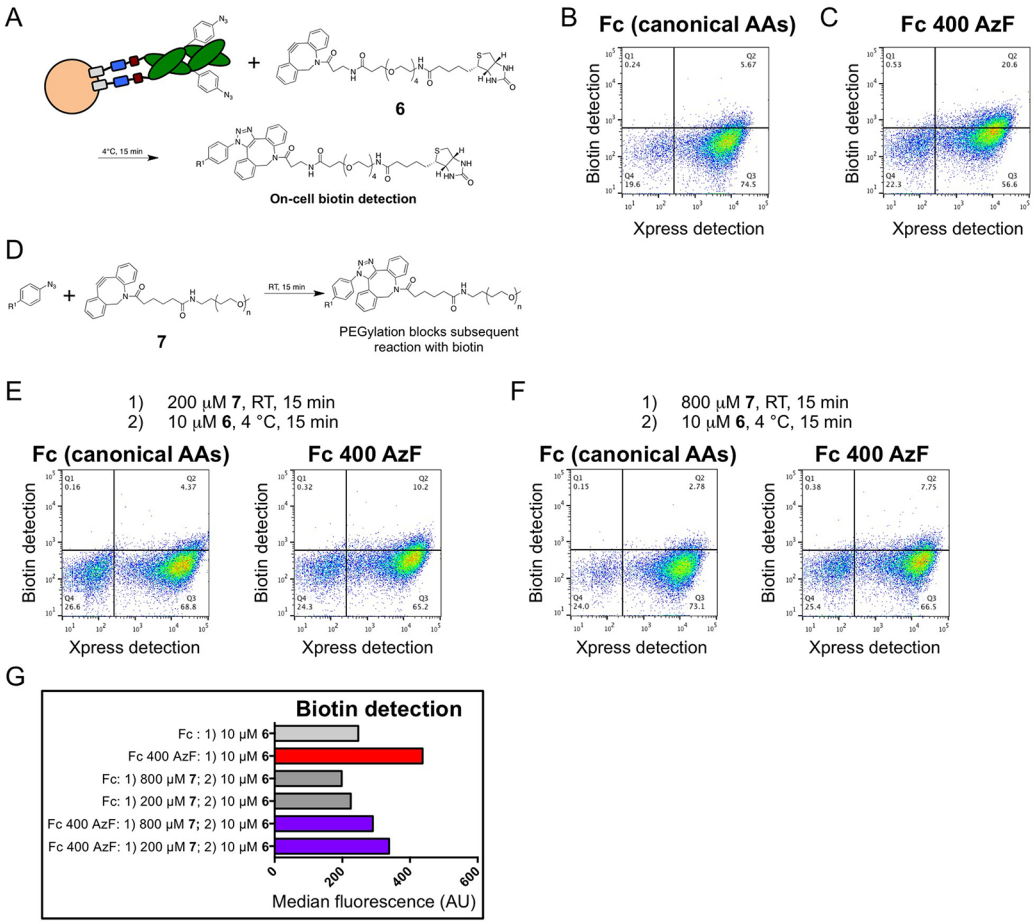

Fig. S3. Strain-promoted azide-alkyne cycloaddition (SPAAC) on the yeast surface. (**A**) Schematic representation of SPAAC reaction between yeast displaying AzF-containing Fcs and dibenzylcyclooctyne-biotin **6**. (**B**), (**C**) Flow cytometric detection of biotin after reactions with yeast displaying wild-type Fcs (**B**) or Fcs containing an AzF substitution at position 400 (**C**). (**D**) Schematic representation of two-step detection of reaction products on the yeast surface using SPAAC. (**E**), (**F**) SPAAC reactions were used to perform functionalization with dibenzylcyclooctyne-PEG **7** at 200 μM (**E**) and 800 μM (**F**), which cannot be detected with affinity reagents. A second SPAAC reaction with **6** and subsequent biotin detection revealed that reactions with 800 μM **7** (**F**) result in cells exhibiting near-background levels of fluorescence. (**G**) Median fluorescence values of samples subjected to two-step SPAAC reactions. R^1: Fc-yeast; RT: room temperature.

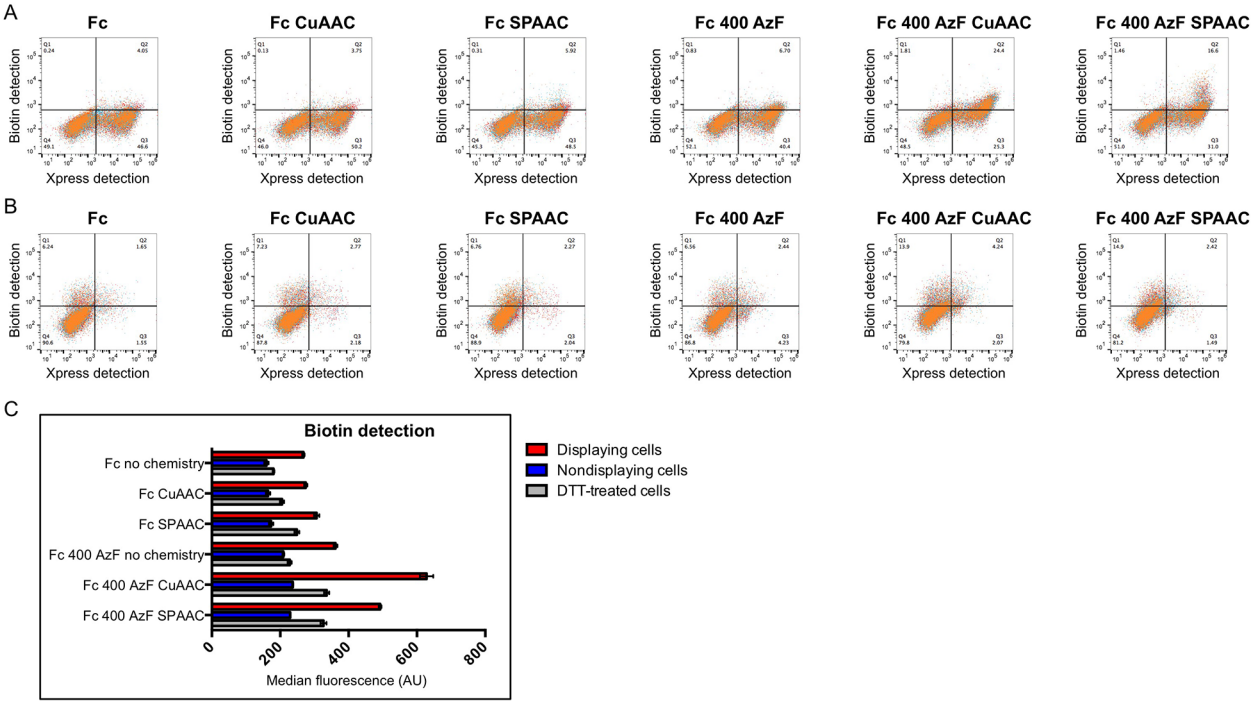

Fig. S4. Dithiothreitol-based removal of Fcs from the yeast surface before and after click chemistry. (**A**) Flow cytometric detection of biotin in Fc and Fc 400 AzF samples after no reaction, CuAAC, and SPAAC prior to dithiothreitol (DTT) reduction. Plots shown here are overlays of each sample evaluated in triplicate experiments. (**B**) Flow cytometric detection of biotin in Fc and Fc 400 AzF samples after no reaction, CuAAC, and SPAAC following DTT reduction. Plots shown here are overlays of each sample evaluated in triplicate experiments. (**C**) Median fluorescence values of displaying and nondisplaying cells from samples depicted in (**A**) and DTT-treated samples depicted in (**B**).

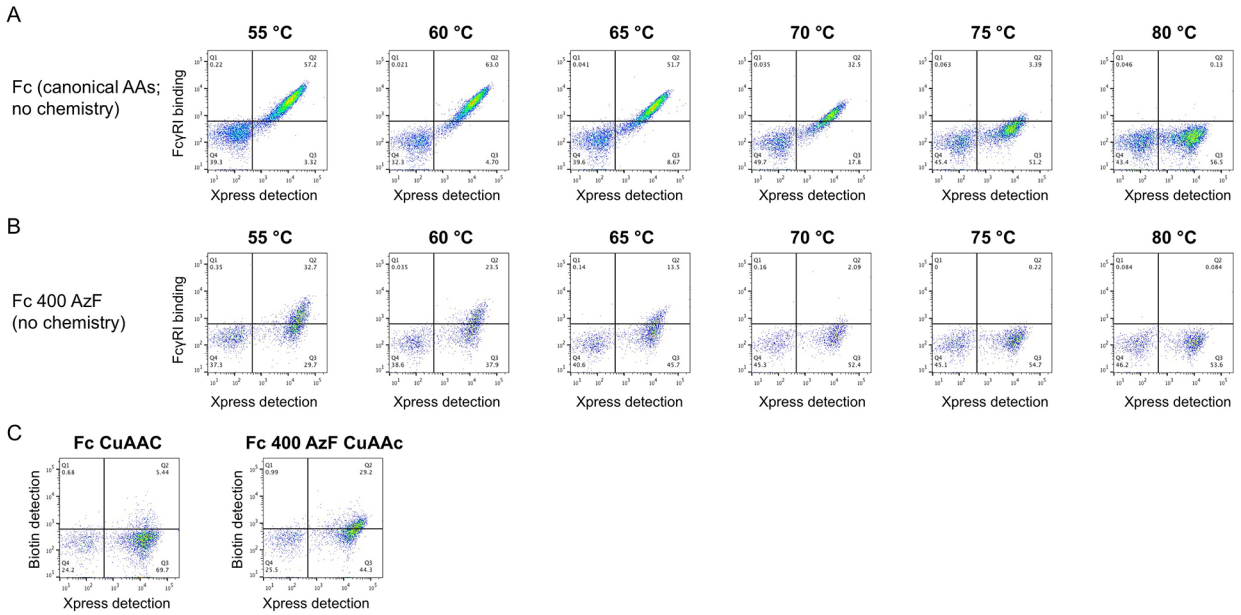

Fig. S5. Representative flow cytometry plots and confirmation of successful CuAAC in thermal denaturation samples. (**A**), (**B**) Representative samples from thermal denaturation experiments with yeast cells displaying wild-type Fcs (**A**) and Fcs containing an AzF substitution at position 400 (**B**). The temperature series shown here were performed on samples that did not undergo CuAAC. The disparities in the colors of plotted data observed in (**A**) and (**B**) are the result of different numbers of events recorded during data acquisition and not changes in cell or protein properties. (**C**) Flow cytometry detection of biotin after CuAAC with cells displaying wild-type Fcs or Fcs containing an AzF substitution at position 400.

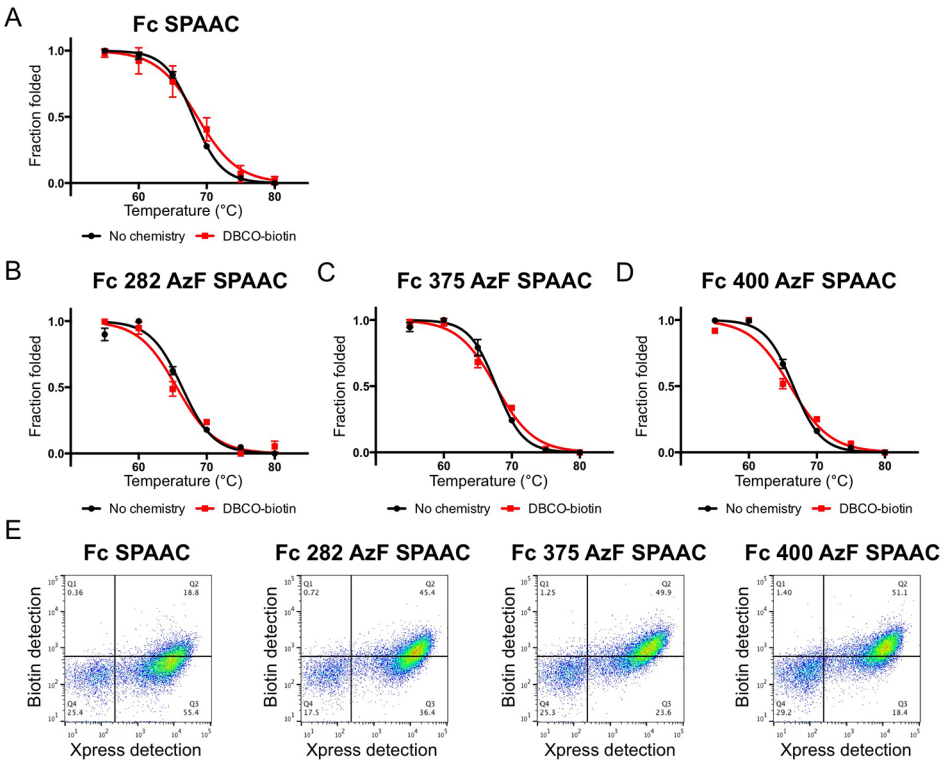

Fig. S6. Thermal denaturation experiments with samples subjected to SPAAC with **6**. (**A**)–(**D**) SPAAC thermal stability studies with wild-type Fcs (**A**) and Fcs containing AzF substitutions at positions 282 (**B**), 375 (**C**), or 400 (**D**). Treatment with **6** does not affect the thermal stability of these samples. (**E**) Flow cytometric detection of biotin after SPAAC with cells displaying wild-type Fcs or Fcs containing an AzF substitution at the indicated position.

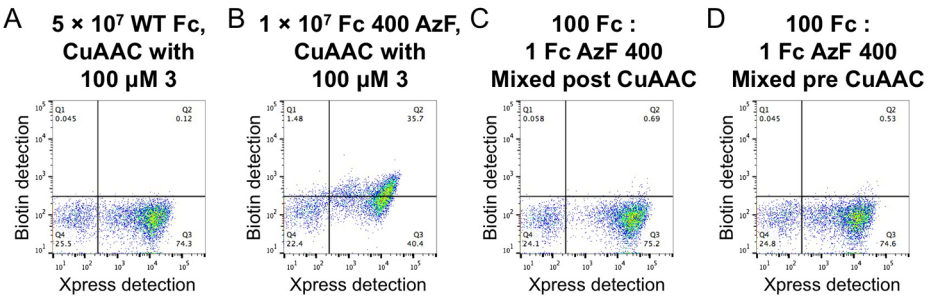

Fig. S7. Representative control experiments performed during fluorescence-activated cell sorting experiments. (**A**), (**B**) CuAAC reactions performed with (**A**) 50 million cells displaying wild-type Fcs or (**B**) 10 million cells displaying Fcs containing an AzF substitution. The higher concentration of **3** used here was empirically determined. Increasing the concentration of **3** did not increase nonspecific biotinylation of wild-type Fcs in 50 million-cell samples (the total size of all sorted samples) or change the fluorescence properties of AzF-containing Fcs in 10 million-cell samples (20X more cells than the number of cells displaying AzF-containing in 100:1 mixtures) compared to the 20 μM concentration of **3** used with 2 million cells in analytical experiments. These controls confirm that CuAAC works efficiently with higher cell numbers and cell densities than those used during analysis. (**C**), (**D**) Flow cytometric analysis of mixtures of yeast displaying wild-type and AzF-substituted Fcs. CuAAC in (**C**) was performed on separate samples of cells displaying wild-type and AzF-substituted Fcs (shown in (**A**) and (**B**), respectively). Only after CuAAC were portions of the samples mixed and labeled for flow cytometry. CuAAC in (**D**) was performed after mixing yeast displaying wild-type and AzF-substituted Fcs; this panel is identical to the "100 Fc : 1 Fc 400 AzF" panel in Figure 4A and is shown for reference. The preparations in (**C**) and (**D**) give rise to indistinguishable staining patterns, confirming the selectivity of CuAAC for cells displaying AzF-containing proteins even in a background consisting of a large excess of cells displaying wild-type constructs. WT: wild-type.